A Scalable Platform for Integrating Horizontal Nanochannels with Known Registries to Microchannels

Babak Nikoobakht*

Surface and Microanalysis Science Division, National Institute of Standards and Technology, 100 Bureau Drive, Mail Stop 8372, Gaithersburg, Maryland 20899

Received July 11, 2008. Revised Manuscript Received September 19, 2008

Controlling the location and physical orientation of nanobuilding blocks in assemblies of nanodevices become challenging tasks when it comes to the use of "bottom-up" chemical approaches for nanodevice fabrication. Here, a strategy is reported for in situ fabrication of horizontal nanochannels, which allows control over their orientation and average pore size to an unprecedented range of ∼5−20 nm. Using this approach, we selectively fabricated nanochannels with controlled average pore sizes at known positions on a sapphire surface. Equally important, nanochannels, either single or group, are addressable photolithographically and integrable to microchannels without the use of any high resolution lithography. This technique uses horizontal ZnO nanowires (NWs) as a sacrificial template and could provide the capability of fabrication of complex micro- and nanofluidic platforms. Cross-sections of nanowires and nanochannels are prepared via a focused-ion beam and examined by electron microscopy and energy-dispersive X-ray spectroscopy.

Introduction

In the ongoing device miniaturization efforts, microchannels and nanochannels have attracted a considerable amount of attention because of the rich physics and chemistry of matter in confined spaces and the potential emergence of new technologies.[1,2] Surface-modified nanochannels are of interest in molecular separation and chemical sensing[3−6] and are ideal structures for probing and analyzing species in very small volumes such as bioentities in a cell. In integrating nanochannels into existing microfluidic platforms, there are few basic requirements that need to be met; fabrication processes should be cost-effective, scalable, compatible with optical lithography, and reproducible. A variety of strategies have been used for fabrication of nanochannels. For example, top-down methodologies have been used to make micrometer-wide channels with sub-100 nm thicknesses,[2] multiple nanochannels 100 nm wide and up to 500 nm deep using interference lithography,[7] and single nanochannels using sacrificial electrical spinning fibers with pore diameters of about 110 nm.[8]

Fabricating channels with dimensions less than 25 nm becomes more challenging. This is, in part, due to the limitations of an electron beam writing tool or line-edge-roughness created during the fabrication process using, for instance, a reactive ion etching (RIE) tool. In nanochannel fabrication, such effects create comparable edge roughness to the pore size of the nanochannel. However, methods have been reported recently that reach this size regime, at least in one dimension. For instance, single nanochannels made by chemical mechanical polishing and thermal oxidation[9] in which the channel width is about 25 nm and its depth is about 100 nm. More recently using a combination of anisotropic etching and edge patterning, long nanochannels 11 nm in width and 50 nm in depth were reported.[10] The prepared nanochannels using top-down approaches usually produce rectangular-shaped pores. Along the length of such nanochannels, variation in the pore shape, thickness, and wall roughness could become disadvantageous because of the possibility of nanochannel blockage during the fabrication process.

In addition to the top-down strategies, there are chemical approaches, such as "template" based methods, by which nanotubes with sub-100 nm pore sizes have been prepared. A popular template has been the porous aluminum oxide membrane, by which silicon oxide nanotubes with diameter range of 30−50 nm have been made.[11,12] Silicon oxide nanotubes have also been made using standing silicon NWs

* Corresponding author. E-mail: babakn@nist.gov. Tel: (301) 975 3230. Fax: (301) 926 6689.

(1) Tegenfeldt, J. O.; Prinz, C.; Cao, H.; Huang, R. L.; Austin, R. H.; Chou, S. Y.; Cox, E. C.; Sturm, J. C. *Anal. Bioanl. Chem.* **2004**, *378*, 1678.
(2) Abgrall, P.; Gue, A.-M. *J. Micromech. Microeng.* **2007**, *17*, R15.
(3) Lee, S. B.; Mitchell, D. T.; Trofin, L.; Nevanen, T. K.; Suderlund, H.; Martin, C. R. *Science* **2002**, *296*, 2198.
(4) Fan, R.; Karnik, R.; Yue, M.; Li, D.; Majumdar, A.; Yang, P. D. *Nano Lett.* **2005**, *5*, 1633.
(5) Kasianowicz, J. J.; Brandin, E.; Branton, D.; Deamer, D. W. *Proc. Natl. Acad. Sci. U.S.A.* **1996**, *93*, 13770.
(6) Sun, L.; Crooks, R. M. *J. Am. Chem. Soc.* **2000**, *122*, 12340.
(7) O'Brien II, M. J.; Bisong, P.; Ista, L. K.; Rabinovich, E. M.; Garcia, A. L.; Sibbett, S. S.; Lopez, G. P.; Brueck, S. R. J. *J. Vac. Sci. Technol., B* **2003**, *21*, 2941.
(8) Czaplewski, D. A.; Kameoka, J.; Mathers, R.; Coates, G. W.; Craighead, H. G. *Appl. Phys. Lett.* **2003**, *83*, 4836.
(9) Lee, C.; Yang, E. H.; Myung, N. V.; George, T. *Nano Lett.* **2003**, *3*, 1339.
(10) Liang, X.; Morton, K. J.; Austin, R. H.; Chou, S. Y. *Nano Lett.* **2007**, *7*, 3774.
(11) Martin, C. R. *Chem. Mater.* **1996**, *8*, 1739.
(12) Zhang, M.; Bando, Y.; Wada, K.; Kurashima, K. *J. Mater. Sci. Lett.* **1999**, *18*, 1911.

10.1021/cm801893z
Published on Web 12/05/2008

as a template via a thermal oxidation-etching process.[13] The formed nanotubes at high temperature retain the orientation of the original silicon nanowires and have relatively thick and rigid walls, whereas those at room temperature may contain pores in their walls which make them less favorable. In applications, typically, such nanotubes need to be removed from their templates and dispersed on another surface or into a solution. In nanofluidic applications using these nanotubes, multistep high-resolution lithography combined with optical lithography is necessary to access the nanotubes.[14]

In the use of horizontal ZnO NWs as template, there are two significant benefits: first, the produced nanochannels are addressable photolithographically; second, conventional microfabrication techniques are applicable. In the horizontal growth of a semiconductor nanowire using the vapor−liquid−solid mechanism,[15] a gold nanodroplet acts as the nucleation site on *a*-plane sapphire.[16] As the gold nanodroplet is fed by Zn and Oxygen precursors in the gas phase, ZnO crystal grows on the sapphire surface and pushes the gold droplet forward. In this process, the location and NW growth direction are controlled. Previously, we used these advantages and developed a method for large scale fabrication of NW field-effect transistors.[17] In this work, benefiting from control over location and direction, horizontal ZnO NWs are used as templates to fabricate nanochannels that have not been prepared previously within inorganic materials via existing fabrication technologies.

Experimental Section

Patterning Sapphire Surface with Gold. Briefly, using optical lithography protocols square patterns of gold with 2 μm in dimension are formed on a *a*-plane sapphire[17] and subsequently annealed at 700 °C in Ar atmosphere. In the annealing process typically gold coated sapphire substrate is inserted into a clean quartz tube (inside a tube furnace), followed by a purge with Ar or N_2 gas for 15 min. The gas flow rate is kept at 0.5 SLPM. The annealing steps include a slow ramp from room temperature to 700 °C within 70 and 5 min of dwell time at 700 °C. This is followed by a furnace self-cool down stpe to room temperature.

Growth of Nanowires. Horizontal ZnO NWs are grown on predefined locations via a phase transport process using patterns of gold nanodroplets as nucleation sites.[17,19,20] ZnO/graphite mixture (0.15 g, 1:1 mass ratio, Alfa Aesar) is loaded on a Si substrate and positioned at the center of an inner tube (13 cm length, 1.9 cm inner diameter). Subsequently, this tube containing a sapphire substrate is inserted into a tube furnace such that the mixed powder is placed at the center of an outer tube (80 cm length, 4.9 cm inner diameter). The tube furnace temperature is set at 900 °C (with a ramp rate of 110 °C/min.) for 10 min under 0.6 standard liters per minute (SLPM) flow of 99.99% Ar gas.

(13) Fan, R.; Wu, Y.; Li, D.; Yue, M.; Majumdar, A.; Yang, P. *J. Am. Chem. Soc.* **2003**, *125*, 5254.
(14) Karnik, R.; Fan, R.; Yue, M.; Li, D.; Yang, P.; Majumdar, A. *Nano Lett.* **2005**, *5*, 943.
(15) Wagner, R. S.; Ellis, W. C. *Appl. Phys. Lett.* **1964**, *4*, 89.
(16) Nikoobakht, B.; Michaels, C. A.; Vaudin, M. D.; Stranick, S. J. *Appl. Phys. Lett.* **2004**, *85*, 3244.
(17) Nikoobakht, B. *Chem. Mater.* **2007**, *19*, 5279.
(18) Nikoobakht, B.; Eustis, S. **2008**, submitted.
(19) Huang, M. H.; Mao, S.; Feick, H.; Yan, H.; Wu, Y.; Kind, H.; Weber, E.; Russo, R.; Yang, P. *Science* **2001**, *292*, 1897.
(20) Yazawa, M.; Koguchi, M.; Hirutna, K. *Appl. Phys. Lett.* **1991**, *58*, 1080.

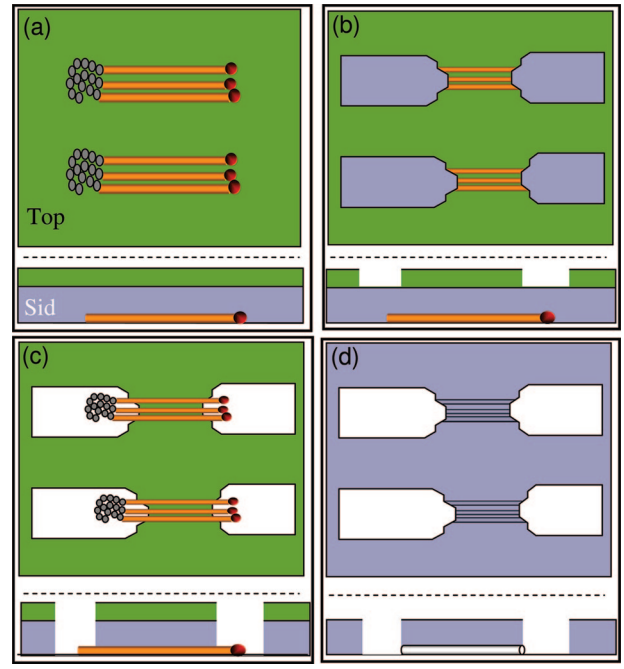

Figure 1. Fabrication steps of horizontal silicon oxide nanochannels, schematically, viewed from top and side: (a) Growth of horizontal ZnO NWs, followed by deposition of a 1 μm thick silicon oxide layer (gray) on substrate, and finally overcoating with a photoresist (green). (b) Developing the microchannel patterns in the photoresist that are overlapped with the two ends of NWs. (c) RIE of the exposed areas in the photoresist until the NWs and sapphire surface are exposed. (d) Formation of nanochannels by ZnO reduction and its release in H_2/Ar atmosphere.

Sample Preparation for Reactive Ion Etching and Formation of Nanochannels. The silicon oxide layer is coated with a 3 μm thick photoresist (Shipley SPR 220−7.0, which contains propylene glycol monomethyl ether acetate, mixed cresol novolak resin, fluoroaliphatic polymer esters, diazo photoactive compound and cresol). (Certain commercial equipment, instruments, or materials are identified in this paper to adequately specify the experimental procedure. In no case does such identification imply recommendation or endorsement by the National Institute of Standards and Technology, nor does it imply that the materials or equipment identified are necessarily the best available for the purpose.) Spin coating is done in two steps: (a) 5 s, 400 rpm, acceleration of 252, (b) 45 s, 4500 rpm, acceleration of 10164. This thickness is chosen to ensure that during the silicon oxide etching step, there remains enough photoresist to avoid etching the rest of the silicon oxide layer. The photoresist residue (postetch) is removed by EKC-265 at 80 °C (this solvent is corrosive and contains: 2-(2-aminoethoxy) ethanol, hydroxylamine, catechol). In the final step, ZnO NWs are etched out of the silicon oxide layer by sample annealing in a 6% H_2/Ar atmosphere (flammable mixture) at 600 °C for 50 min.

Cross-Section Preparation and Electron Microscopy. Cross-sections of nanochannels and ZnO nanowires are prepared by a FEI DualBeam instrument, a combination of a focused ion beam (FIB) and a scanning electron microscope (SEM). The electron micrographs of the cross-sections are obtained using a SEM in the scanning transmission electron microscopy (STEM) mode at acceleration voltage of 30 keV.

Results and Discussion

The strategy for making nanochannels is illustrated in Figure 1. In the first step (part a), horizontal ZnO NWs are grown selectively on sapphire surface from gold nanodroplets

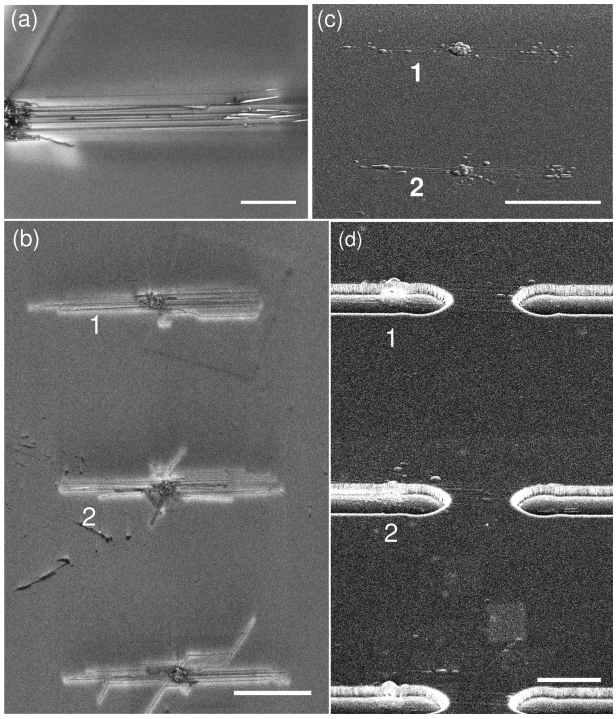

Figure 2. SEM images of different steps of nanochannel fabrication. (a) A group of horizontal ZnO NWs grown on *a*-plane sapphire before any treatment. Scale bar: 2 μm. (b) Selective growth of horizontal NWs where gold pads are deposited. Scale bar: 8 μm. (c) Two groups of silicon oxide-coated ZnO NWs. Scale bar: 10 μm. (d) Overlap of microchannels on groups of nanochannels after silicon oxide RIE and ZnO reduction (Supporting Information, Figure S4). Scale bar: 4 μm. In parts (b, c), two groups of NWs labeled 1 and 2 are shown at different stages of the fabrication. This illustrates the traceability and ability to link nanochannels to their corresponding NWs.

that are deposited photolithographically. Next, the entire substrate is coated with a thick silicon oxide layer (gray color), followed by a photoresist coating (green color). In part b, patterns of microchannels are produced in the photoresist using a second round of photolithography. Fiducial marks are used to ensure that microchannels overlap with the two ends of the embedded horizontal NWs. This step is followed by RIE (part c) to transfer the photopatterns to the oxide layer underneath the photoresist. After the photoresist removal (part d), ZnO is etched out using a gas phase etching process and nanochannels are formed at the interface of silicon oxide layer and sapphire substrate.

A SEM image of a group of horizontal ZnO NWs grown from a single gold pad on *a*-plane sapphire is shown in Figure 2a. The selective growth of groups of NWs with known locations on a larger scale is also shown in Figure 2b (see the Supporting Information, Figure S1). The unique growth direction of NWs, has been attributed to a lower lattice mismatch and lattice strain in $[1\bar{1}00]$ direction.[16,18] In this figure, it is also seen that some NWs tend to change their direction, which is due to the organic residues of the photoresist on the sapphire surface. When a growing NW encounters an obstacle on the surface, it changes its direction and often takes a random growth direction. Next, a 1 μm thick silicon oxide layer is deposited on the entire surface using a plasma enhanced chemical vapor deposition (PECVD) process. Figure 2c displays two groups of overcoated ZnO NWs, which are still observable from the topography of the

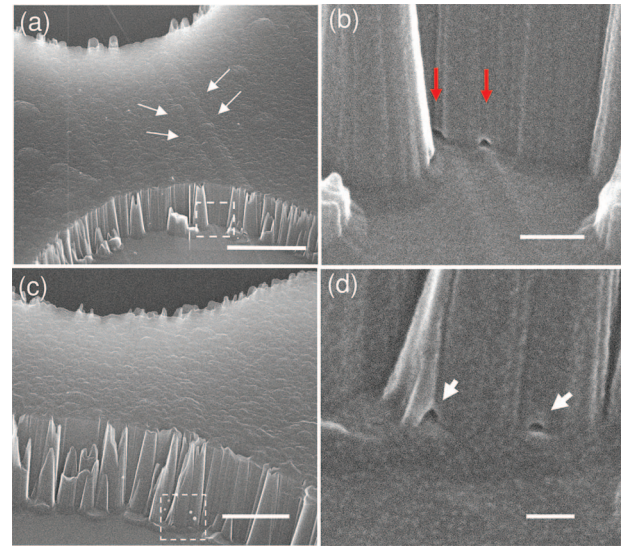

Figure 3. (a) Shows a close view of a gap between two microchannels etched in silicon oxide. White arrows show traces of the formed nanochannels in the silicon oxide layer. The marked area contains entrances to two nanochannels. Scale bar, 1 μm. (b) Red arrows point at the entrances of the nanochannels described in part (a). Scale bar: 100 nm. (c) Side view of a submicrometer gap between two microchannels that contains two nanochannels. The marked area contains the entrances to two nanochannels. Scale bar, 500 nm. (d) The entrances of the nanochannels described in part (c) with an average diameter of 12 nm. Scale bar, 50 nm.

oxide surface. In images b and c in Figure 2, the sites labeled 1 and 2 refer to identical groups of NWs before and after coating with the oxide layer, respectively. The oxide layer is then coated with a 3 μm thick photoresist and subsequently patterned with microchannels such that the gap between them overlaps with the ZnO NWs (schematically shown in Figure 1b). To expose the two ends of the NWs, RIE is performed to etch out the oxide layer from the patterned regions. The etching is continued until the etched areas reach the sapphire substrate. After removal of the postetch photoresist residue, the resulting structures are treated in a H_2/Ar atmosphere to completely etch out the ZnO NWs. Comparison of morphologies of the micro- and nanochannels before and after ZnO removal, indicates that the hydrogen treatment at 600 °C does not change their morphology (see the Supporting Information, Figures S2 and S3). Figure 2d illustrates the micro-nanochannel integration and the ease of parallel targeting of groups of nanochannels (see also the Supporting Information, Figure S4). This method allows fabrication of densely packed and numerous addressable nanochannel-microchannels enabling development of platforms and templates for more complex nanofluidic designs or nanodevice fabrications. One advantage of this platform is the ease of locating nanowires or nanochannels of interest. Another advantage is the ability to trace back nanochannels to their original nanowires. This simplicity of mapping is shown for groups of NWs and nanochannels labeled 1 and 2 in Figure 2b−d (see the Supporting Information, Figures S4 and S5). Thus to find out about the height or shape of some specific nanochannels, they can be linked back to their original NWs (see the following sections).

Figure 3a illustrates a typical product of this process, where two microchannels are bridged by two nanochannels that are

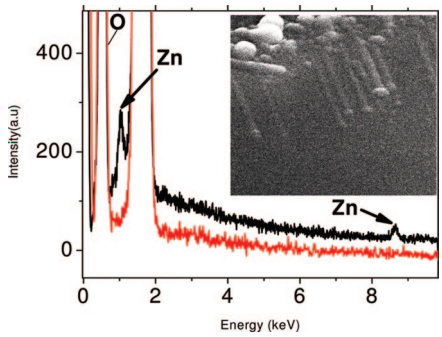

Figure 4. EDS spectra of ZnO NWs and nanochannels obtained at 20 keV. Black curve: Spectrum of ZnO NWs coated with 1 μm of silicon oxide. Red spectrum: Spectrum of the same region after etching out the ZnO. Inset shows a SEM image of the examined region. Peaks corresponding to Zn element have disappeared after the ZnO etching process.

shown with arrows. The two nanochannel inlets are located in the marked area in this figure and their side view with a higher magnification is shown in Figure 3b (Figure S6). An example of a short length nanochannel is shown in Figure 3c, where the channel length is <1 μm. The marked area in this figure is shown with a higher magnification in Figure 3d, where the entrances of the two nanochannels can be seen. In this case, the average nanochannel diameter was measured to be 12 nm. The maximum nanochannel length depends on the length of the original NW and could be extended to 40 or 50 μm. The spacing between the nanochannels is not controlled at this point and is determined by the spacing between the gold nanodroplets.

To confirm the complete release of ZnO from the silicon oxide nanochannels, we carried out EDS analysis at 20 keV on a group of NWs, coated with 1 μm thick oxide, before and after their etching. Figure 4 shows the black and red spectra corresponding to the over coated ZnO NWs before and after ZnO removal, respectively. It can be seen that the two Zn peaks have disappeared after the hydrogen treatment. The duration of the etching process was intentionally extended to 50 min to ensure a complete release of ZnO.

Nanochannels are further characterized by examining their cross-sections and comparing them with those of the over-coated ZnO NWs before the chemical etch. The electron transparent cross-sections are prepared using a FEI Dual-Beam.[21] The electron micrographs of the cross-sections are obtained using the SEM in the STEM mode. Figure 5a, shows a cross-section of a group of ZnO NWs with 7 nm average diameter before ZnO reduction in H_2/Ar atmosphere (diameter distribution shown in Figure S8a). The bright dots at the interface between sapphire (bottom layer) and silicon oxide (top layer) are ZnO NWs. Figures 5b shows a cross-section of a different group of NWs after the ZnO removal. The group of NWs that was used to make these nanochannels

(21) The protocol used for preparing sub-100 nm cross-sections is a modified form of the following reference: (a) Giannuzzi, L. A.; Kempshall, B. W.; Anderson, S. D.; Prenitzer, B. I.; Moore, T. M. F. *Analysis Techniques of Submicron Defects: 2002 Supplement to the EDFAS Failure Analysis Desktop Reference*; ASM International: Materials Park, OH, 2002; pp 29−35.

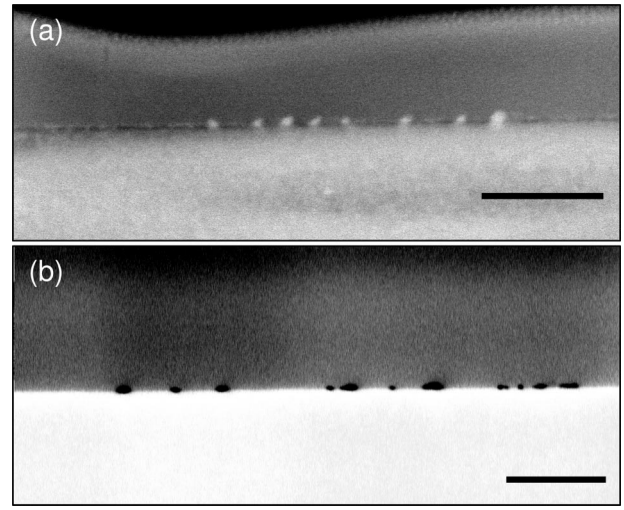

Figure 5. STEM images of cross-sections of silicon oxide-coated ZnO NWs before and after formation of nanochannels. (a) Cross-section of ZnO NWs with an average diameter of about 7 nm measured by AFM before cross-sectioning (size distribution is shown in Figure S8a). Scale bar, 300 nm. (b) Cross-section of formed nanochannels at the silicon oxide−sapphire interface after ZnO reduction in H_2. Scale bar, 300 nm.

is shown in the Supporting Information, Figure S7b. As stated earlier, one of the benefits of this method is that nanochannels can be traced back exactly to their original NWs for their morphology and height information. In Figure 5a, examining the cross-sections of areas that contained ZnO shows that the bright spots associated with the ZnO are turned to hollow features, shown in Figure 5b, demonstrating the removal of the ZnO (see the Supporting Information, Figure S7a). Progressive FIB slicing and viewing with SEM along the length of the nanochannel further confirms the removal of ZnO. These nanochannels typically have semicircular profiles with sapphire as their bottom surface. On the basis of the AFM examination, the diameters of NWs remains constant along the length of NWs; therefore, variation in the pore size along the nanochannel length is minimal.

The number of nanochannels per site depends on the number of pre-existing ZnO NWs grown from a gold pad. In our experiments, because of the resolution of the photolithography tool (1 μm smallest feature), the size of the deposited gold features are set to about 2 μm. As a result, typically, few NWs (2 to 10) are grown at each site. However, by reducing the gold pad size, it is possible to lower the number of gold nanodroplets and subsequently the number of grown NWs to one, resulting in one nanochannel at a given site. Although at this point, using this technique, single nanochannels have not been prepared on a large scale, it is possible to make such devices with a low yield by minimizing the number of gold nanodroplets at each site. This is done by immersion of gold patterned sapphire into a gold etching solution of $KI/I_2/H_2O$ (8 g:2 g:40 mL) for 10−30 s. During gold nanodroplet formation, both large and small size droplets are formed, from which only the larger ones survive the gold etching process. This process results in a lower number of gold droplets at each site, but further increases their interparticle spacing. Figure 6a shows a device containing a single nanochannel between two microchannels. It also shows some nanochannels that are in other directions.

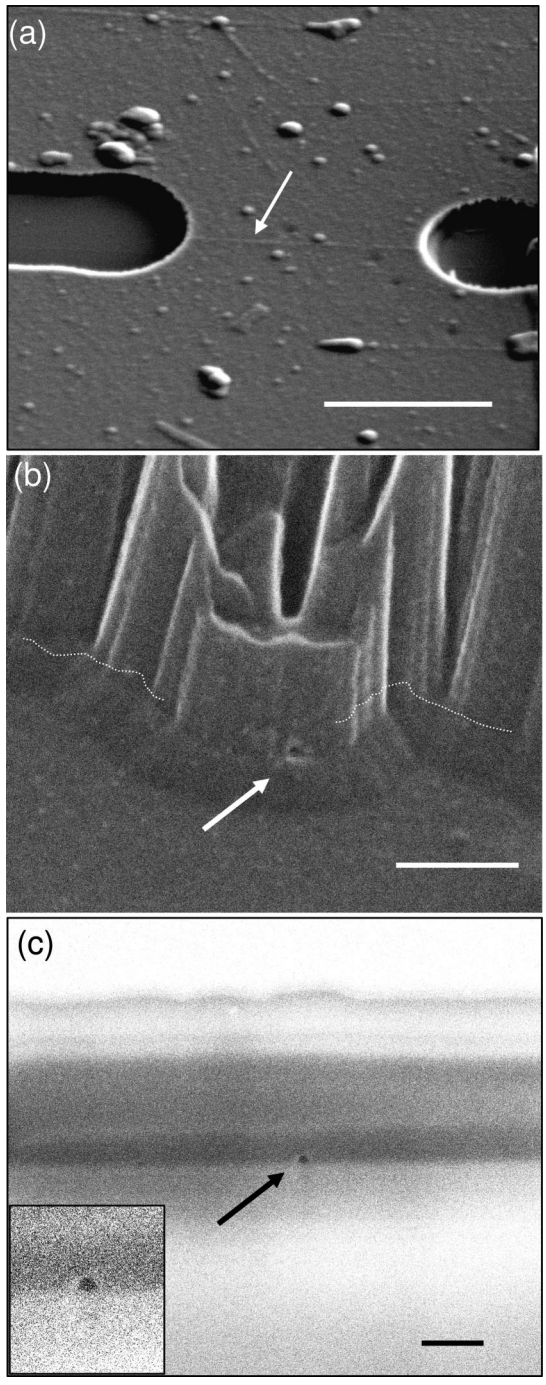

Figure 6. (a) Nanodevice containing only a single nanochannel marked with an arrow. Scale bar, 500 nm. (b) The entrance of the single nanochannel shown in part (a) with a SEM-estimated pore size of about 10 nm. Scale bar, 100 nm. The dashed line shows the silicon oxide/sapphire interface. (c) Represents cross-section of a different device containing one nanochannel. The estimated pore size is about 25 nm. Inset shows a magnified view of the pore. Scale bar, 200 nm.

The deviation in nanochannel orientation is related to the change in growth direction of NWs. This change is due to the photoresist residual on sapphire surface as previously described. Therefore surface cleaning is a key factor in obtaining unidirectional NWs and nanochannels. Figure 6b shows a side view of one of the nanochannel ends. In this case the pore size is estimated to be about 10 nm. Figure 6c and inset illustrate a cross-section of a different device containing a single nanochannel, with a pore size of about 25 nm measured by SEM. In estimating the average nanochannel diameter, atomic force microscopy (AFM) was used to estimate the NW thickness instead of direct nanopore size measurements from SEM.

Average pore sizes of nanochannels are adjusted by controlling the average diameters of the nanowires, which are tuned by the size of gold nanodroplets. In this work, gold pads with 6, 11, and 14 nm thickness, deposited on a sapphire substrate, are used for growth of NWs. Before the growth process, the gold pads are thermally annealed resulting in formation of gold nanodroplets with a certain size distribution (see the Supporting Information, Figure S8). This size distribution will also be reflected in that of the ZnO NWs and subsequently in the size distribution of the fabricated nanochannels. We have measured average nanochannel pore sizes of 7, 12, and 15 nm corresponding to the three deposited gold thicknesses of 6, 11, and 14 nm. Nanochannel height statistics were obtained from the AFM height measurements on NWs before their transformation to nanochannels (see the Supporting Information, Figure S8). These measurements show a 30−40% broadening in diameter of NWs relative to the distribution mean value. The ability to fabricate nanochannels with different pore sizes at selected locations of a substrate and in a parallel process is a new capability that is offered by this method. In using thicker gold films to increase the diameters of nanochannels, the diameter distribution seems to become bimodal. This is most likely due to the formation of two size distributions of gold nanodroplets during the thermal annealing of the thicker gold film (see the Supporting Information, c and e in Figure S8). This broadening could be narrowed by forming more uniform gold nanodroplets via an improved annealing step or use of colloidal gold nanoparticles that have a better size distribution.[16,22] The developed template provides a significant tunability with respect to nanochannel material and design. For instance, fabricating nanochannels with different wall materials at different locations of a chip is expected simply by overcoating ZnO nanowires with different materials than silicon oxide.

Conclusion

The developed method is shown to have the advantage of a "top-down" technique in which nanochannels are built where they need to be. On the other hand, it provides the fine control of a "bottom-up" chemical approach on characteristics of a nanochannel such as dimensions and shape. In this work, it was shown that by controlling the thickness of the deposited gold film, the average size of the nanochannels could be controlled. In fabricating groups of NWs and nanochannels, there is a limited ability to control their spacing. Nonetheless, the location of groups of nanochannels could be controlled with a good resolution. Unlike the case for suspended nanotubes made by other techniques, horizontal nanochannels are readily accessible by microchannels using conventional microfabrication methods without the need for physical ma-

(22) Gudiksen, M. S.; Wang, J.; Lieber, C. M. *J. Phys. Chem. B* **2001**, *105*, 4062.

nipulation, transfer, or complex fabrication steps. This template not only allows production of very small pore sizes down to few nanometers but also enables formation of nanochannels with different diameters at designated locations on a substrate, an ability that becomes important in the design of more complex nanofluidic platforms.

Supporting Information Available: Complementary SEM images, nanowire/nanochannel height measurements, and corresponding SEM cross-sections (PDF). This material is available free of charge via the Internet at http://pubs.acs.org.

CM801893Z